

Molecular Dynamics Simulation of Phase Transitions in Binary LJ Clusters

Adem TEKİN, Mine YURTSEVER*
*Istanbul Technical University,
80626 Maslak, İstanbul-TURKEY*

Received 15.11.2001

The structures of small clusters are studied extensively by classical simulation methods because of their interesting thermodynamic behavior. In this work, we study the thermodynamic properties of binary mixtures of noble gas atoms. Interatomic interactions are defined by 6-12 Lennard-Jones (LJ) potential. Starting from the global minimum of the potential energy surfaces, the systems are heated by increasing the total energy until melting occurs. The melting is observed by monitoring the Lindemann factor. The effects of the relative sizes of A and B atoms and the interaction strength of A-A, A-B, and B-B on the melting temperature of clusters containing 50% of each component is analyzed by using constant energy (NVE) molecular dynamics simulation. It is observed that the heterogeneous clusters melt at lower temperatures as long as the relative interactions are of similar order. Melting points do not follow a systematic trend with size, mostly due to the unusual stability of certain size clusters.

Introduction

In recent years, there has been a great growth of research on atomic and molecular cluster systems. The development of new experimental techniques¹⁻⁴ allow the spectroscopic characterization of clusters together with the development of new algorithms and increased speed of computers making the realistic simulations of clusters possible allow a better understanding of clusters.

Clusters form a bridge between the microscopic world of individual atoms or molecules and the macroscopic world of bulk materials. Many researchers have performed studies to identify variations in the properties of clusters as a function of cluster size, developing an improved microscopic-level understanding of hydrogen bonding⁵ and other solvation phenomena⁶. Clusters also provide a information between topology of the potential energy surface and the underlying dynamics and thermodynamics at a level of detail that is not possible for bulk systems. Furthermore, clusters provide a profound insight into studies like glass formation and protein folding. The number of atoms or molecules in clusters varies from 4-5 to a few hundred. Most of the atoms can be placed on the surface where the local ordering can vary significantly from one atom to another resulting in deviations from homogeneity. This is reflected in the dynamic properties of clusters; especially when they are heated, they change from a solid-like structure to a liquid-like structure where the

*Corresponding author

atoms are loosely bound⁷. Clusters are usually formed either by generating a vapor that contain atoms or molecules and letting them aggregate or by knocking the clusters out of a bulk solid⁸. The effect of temperature is very important for these systems. Clusters have found a great deal of application in material sciences and have widely been used to search for new kinds of chemical reactions. Scientists work on these materials in the hope that they will show certain desired microelectronic, mechanical or catalytic properties.

Clusters, at a definite range of temperature, coexist as solids and liquids and have different melting and freezing points. In the coexistence range, the fraction of solid and liquid clusters depends on the free energies of these two forms. The free energies of clusters vary with temperature change. The density of energy levels and the interplay between energy and entropy result in a cluster having a distinct freezing point, below which only the solid phase is stable, and a distinct melting point, above which only the liquid phase is stable. It is known that at a temperature of about 20 to 30 K, small clusters behave like liquids and large clusters behave like solids. Although atomic or molecular clusters may exhibit solid-like and liquid-like forms that are quite similar to bulk matter in many respects, they have unequal freezing and melting temperatures due to equilibrium between different isomeric forms. In thermal equilibrium, these forms occur in a ratio $k = [\text{solid}]/[\text{liquid}] = \exp(-\Delta F/kT)$, which is fixed by the difference in free energy ΔF between the solid and liquid forms. This is a dynamic equilibrium between the chemical isomers of clusters⁹.

In studying the melting behavior of cluster systems it is essential to ensure that the simulations have attained equilibrium. It has been known for some time that this is much harder to accomplish in some cluster systems than in others, especially when a number of minima separated by large barriers exist. For the melting temperature of clusters in general a simple estimation can be made by using an expression for the free energy of the cluster as a function of particle number¹⁰⁻¹¹. By setting the expressions for the free energies of solid and liquid clusters equal, one obtains the phase equilibrium condition

$$T_m^c(N) = T_m^b - AN^{1/3} \quad (1)$$

where T_m^c is the melting temperature of a cluster of N atoms, T_m^b is the bulk melting temperature, and A is a positive constant. The equation expresses the fact that the melting temperature of the cluster is low when the cluster is small and approaches the bulk melting temperature as the particle number of the cluster increases¹².

Phase coexistence in clusters, the number of coexisting phases, and the occurrence of a solid-liquid transition are related to the peculiarities of the density of states, and in large part to the density of states just of the local minima on that surface. Both these densities can be found numerically, in principle. To do this becomes impractical for systems containing a rather small number of particles; for example, there are approximately 5×10^5 geometrically distinct local minima for Ar_{19} and the number increases exponentially with N , the number of atoms in the cluster. Unfortunately, the high dimensionality of the nuclear configuration space for a cluster means that the number of minima and transition states on the potential energy surface can be astronomically large. Hence, for larger clusters, statistical sampling of simple analytical models can be used to determine densities of states and thermodynamic properties, such as free energies and equilibrium ratios of coexisting phase-like forms¹³.

To identify the complete potential energy surfaces in any cluster system is extremely difficult. If we know the surface, we can, at least in principle, describe the behavior of our system on that surface, for example by using classical mechanics in molecular dynamics simulations or by propagating quantum-mechanical wave packets¹⁴. The most important features that arise on any cluster potential energy surface

are familiar objects in three-dimensional space but are rather harder to visualize in hundreds of dimensions¹⁵.

To define a potential surface we have to know the minima and the saddles that connect them. Local minima form one kind of stationary point on the surface, where all the forces vanish. They are locally stable, in that any infinitesimal change in structure raises the energy. A transition state, on the other hand, corresponds to the highest point along the valley linking two basins. Transition states are also stationary points, but correspond to mechanical instability; i.e. infinitesimal displacements in either direction along the reaction path lower the energy. When one knows the geometry of a system at a saddle, one can determine the entire “reaction path” or path of least energy between the two minima connected by that saddle, simply by applying either of the methods for locating minima, starting with points near the saddle of interest.

Several researchers have extensively studied the potential energy surfaces to find local minima and saddles and have formulated new methods. The methods are now fairly well established. To find minima, the method of steepest descents^{16–17} seems most obvious, but the related, conjugate gradient method is usually much faster¹⁸. Computational algorithms are readily available for both¹⁹, but new and more powerful methods continue to be developed^{20–23}. Two ways have emerged for finding saddles: a faster, “hill-climbing” method^{24–31} and a “skiing-down” method that assures one will find important saddles, the method called “slowest slides”^{32–33}.

Hoare and Pal made the first extensive computations of the minima of rare gas clusters bound by pairwise Lennard-Jones LJ and Morse potentials. Since then, minima have been cataloged for many other clusters, including more rare gas clusters, molecular van der Waals clusters, alkali halides, simple metals, transition metals and semiconductors, as well as some clusters containing dopant or impurity species³⁴.

The lowest energy morphology for clusters bound by pairwise-additive, isotropic forces is determined by a balance between the total number of the nearest-neighbor interactions (stabilizing) and the strain energy (destabilizing). The lowest energy structure is generally based on one of three different morphologies: Mackay icosahedra, decahedra, and closed-packed fragments of regular bulk lattice. Of the three morphologies, the icosahedron maximizes the number of nearest-neighbor contacts but has the highest strain, the truncated octahedron minimizes the strain but has the fewest nearest-neighbour contacts, and the Marks decahedron is intermediate in both categories. Direct comparisons between these structures are not straightforward because complete geometries of high symmetry, which are expected to be particularly low in energy, occur for different numbers of atoms. Hence, for clusters containing less than around 100 atoms, the most stable morphology may change with the addition or removal of a single atom¹⁵.

In bulk material, the first-order melting transition is characterized by solid and liquid phases in contact at the melting point. However, for small systems the energetic penalty for forming an interface is too large for such phase separation to be observed. Instead, it is helpful to think of an isolated individual cluster in terms of a two-state model where in the melting region the cluster behaves like both a solid and liquid. A dynamical equilibrium exists between the two forms with an equilibrium constant that is related to the difference in free energy. If the temperature of the cluster rather than its total energy is under experimental control, the heat capacity has to be positive. Solid-like regions of phase space are associated with restricted motion in low-energy minima. In contrast, liquid-like regions of phase space are associated with passage between a multitude of higher energy, disordered minima. For an isolated cluster at constant total energy, the kinetic energy is larger when the system is associated with a low-energy, solid-like minimum and smaller when it visits liquid-like regions of phase space with higher potential energy. When the total energy is small, the system simply vibrates in a particular low-lying potential well. As the energy rises, the amplitude of the

vibrations increases until eventually the cluster can escape to regions of the potential energy surface that correspond to liquid-like behavior. However, the mean kinetic energy, and hence our measure of the internal temperature, can decrease when this happens.

In this study we would like to look at the melting behavior of heterogeneous clusters using molecular dynamics simulations. The heterogeneity is introduced by changing the sizes of some atoms in the cluster and consequently the packing and hence the thermodynamic stability should be strongly affected. By systematically analyzing the melting of such clusters as functions of the size ratio as well as the relative strength of interactions we aim to understand the structural transitions in binary systems.

Method

The molecular dynamics simulation method is one of the most important statistical mechanical computer simulation techniques used to study many-particle systems^{35–36}. The behavior of a macroscopic system is usually too intricate for analytical statistical mechanical treatment. Computer simulations have been widely used to study the structural and dynamical equilibrium and nonequilibrium properties of chemical systems³⁷. The fundamental aim of the dynamics simulation technique is to define a real system via a mathematical model. Based on this model the time evolution of the particles is then numerically calculated using classical or quantum-mechanical methods. Then the outcome of computer experiments is statistically analyzed. The calculated observables can be directly related to real experiments and to the results from analytic theory. Therefore, computer simulations provide information for both experimental and theoretical studies³⁸.

The MD method³⁹ computes a trajectory of a N-particles system by solving Newton's equations of motion. A system of N-particle is positioned within a cell of fixed volume with the initial positions of the particles exactly known. The initial velocities can be zero or can be obtained from the Maxwell distribution of velocities. The subsequent trajectories of the particles are then calculated by stepwise numerical integration of the classical equations of motion (Newton's equation of motion). The particles are supposed to interact through some prescribed force and at each step the force acting on each particle is calculated from the interaction potential of the system. The length of the time step (about 10^{-15} s, which is shorter than the average time between collisions) usually depends on factors such as temperature, density, particle masses and the nature of the force employed. In MD, the total energy of the system is constant. The states arising at each step of calculation represent a sample from the microcanonical ensemble where the number of particles, volume, and total energy are constant. The solution of the equations of motion is an efficient way of sampling phase space along a surface of constant total energy. The thermodynamic properties of the system are then calculated as averages over time. The LJ model potential, which parameterizes a spherical intermolecular interaction potential in terms of a molecular size parameter, σ , and an attractive potential well-depth constant, ε , is used to represent used the interaction between the atoms in the cluster.

The LJ potential is given as

$$U_{LJ}(r_{ij}) = -4\varepsilon \left(\left(\frac{\sigma}{r_{ij}} \right)^{12} - \left(\frac{\sigma}{r_{ij}} \right)^6 \right) \quad (2)$$

where σ is the hard-sphere diameter and the ε is the energy parameter.

Interactions between unlike atoms in different molecules can be approximated using the venerable

Lorentz-Berthelot mixing rules³⁸. In a binary AB mixture, the cross terms are given by

$$\sigma_{AB} = \frac{1}{2}[\sigma_{AA} + \sigma_{BB}] \quad (3)$$

$$\varepsilon_{AB} = [\varepsilon_{AA} + \varepsilon_{BB}]^{\frac{1}{2}} \quad (4)$$

Calculations

In this work, clusters containing 10-20 atoms are studied. Binary mixtures are obtained by changing the hard-sphere diameters, σ , of approximately half of the total number of atoms so that the number fractions of the different types of atoms are kept around 0.50. The interaction energy parameter ε of the LJ potential is also kept constant during the variation of σ . The initial geometry of various size clusters is taken as one of their minimum energy configurations and initial momenta are assigned in such a way that total momentum is zero. Even for pure LJ clusters, the number of minima along the potential-energy-surface increases exponentially with size. For heterogeneous clusters, this number is even larger. Therefore our starting configuration is possibly not the global but one of the many low-lying local minima. However, our simulations are not strongly affected by the choice of the initial geometry. The basic reason for choosing a minimum configuration and zero momentum as explained below is to generate nonrotating clusters. The rotation of clusters around their moment of inertia axes causes additional complications and they are excluded.⁴⁰ Starting from the minimum energy, the total energy of the system is increased systematically. At each energy the system is brought to equilibrium by 5×10^5 time steps of integration. The number of integration steps is optimized as 500,000 steps. Our program simulates binary LJ clusters, and computes internal temperatures and Lindemann factors for components A and B and the total cluster. A 4-point constant time-step Runge-Kutta integrator is used to solve the coupled equations of motion. In the microcanonical ensemble (simulations are carried out at constant energy) it is important to determine the corresponding temperature. The total internal energy of a system can be written as a sum of kinetic and potential energy contributions and the temperature of the system is proportional to its average kinetic energy, $\langle E_K \rangle$:

$$T = \frac{2}{3N - 6} \frac{E_{kin}}{k_B} \quad (5)$$

where k_B is the Boltzmann constant, and $3N - 6$ represents the total number of internal degrees of freedom. To find the minimum energy configurations of the clusters, David Wales's optimization program⁴¹ OPTIM has been used. The minimum energy configurations obtained this way have been inputted as starting points for the further MD calculations. For small N, the overall rotation of the clusters induces a Coriolis force. The Coriolis force acts on every molecule with a mass and velocity. The effect of this action is a distortion of the molecular trajectory from that of a nonrotating cluster. It is expected that its influence will be greater for smaller than for larger clusters. The influence of the Coriolis force disappears as $1/N$. In our calculations we have used nonrotating clusters in order to eliminate the effects of the rotational motion on melting. To achieve zero angular momentum conditions, the normal modes of the cluster are calculated. Among these modes, three have nonzero linear momentum corresponding to translational motion. Three have zero linear and nonzero angular momentum corresponding to rotational modes. The remaining $3N-6$ modes are vibrational ones and they all have zero angular momentum. The eigenvectors of these modes can be simply used to describe initial momentum distribution of nonrotating clusters.

We have monitored the Lindemann factor in each trajectory to locate the melting point of various clusters. Lindemann factor can be defined in the form of fluctuations of distances between atoms or molecules:

$$\delta = \sum \left(\frac{\langle r_{ij}^2 \rangle - \langle r_{ij} \rangle^2}{\langle r_{ij} \rangle} \right) \quad (6)$$

For $\delta < 0.1$, it is said that the cluster is a solid and for values $\delta > 0.1$ the cluster is a liquid⁴². Phase transition is observed in the region where δ varies between 0.1 and 0.3. Finally, throughout the discussion, we have used generalized units where the mass, ε and σ of one component is assumed to be 1.0. Temperatures are then also defined in these units and they have to be scaled with actual parameters of a LJ system in order to convert into Kelvins.

Results and Discussion

In this work we attempted to understand the melting and phase coexistence behavior for binary LJ clusters as a function of different interatomic forces and atom sizes. Small clusters containing 10-20 atoms are known to exhibit very interesting behaviors upon heating and the physical properties may change drastically when the number of particles is increased slightly. This is related to the drastic changes in the topology of the potential energy surfaces (PES). The complexity of these surfaces seems almost independent of the number of atoms in a cluster and they can be even more complex if the composition and the sizes of the constituent atoms are changed. Finding the global minima and the other low-lying minima are the most important part of cluster studies. The relative stabilities of the low-lying potential energy minima of the clusters are highly dependent on the relative interatomic forces, which can be controlled by changing the potential energy parameters ε_A and ε_B , and the atomic sizes, which can be controlled by the size ratio of the atoms of type A and B. In our calculations the ratio (σ_B/σ_A) is varied between 0.55 and 0.95 for the binary mixtures and the ratio is 1 for the homogeneous clusters. For every parameter set, we used a single trajectory to obtain melting points. Even though the trajectory is integrated for a long time and sampled sufficiently, there exist fluctuations, especially in the phase transition regime. They are expected as the cluster oscillates between two phases (phase coexistence).

In Figure 1, we plotted δ versus average temperature of the homogeneous clusters equilibrated at different energies starting from the global minimum structures. The size of the clusters was changed between 10 and 20. Upon heating the clusters, sudden changes in the slopes of the curves were observed implying phase transitions from solid to liquid structure. The melting temperatures of these systems were obtained from the midpoints of the transition regions. The determined values for the melting temperatures are approximate because of the finite size effect in small clusters. For some N values, the transition curves are different from the others. Some show very sharp transition whereas others have a very broad transition range. In the literature, the 13 atom Lennard-Jones cluster (LJ₁₃) system is one of the most studied cluster systems, especially for argon clusters since it is a representative of clusters with a single funnel PES and has an icosahedra global minimum. It has been noted that a consistent determination of the melting temperature was not possible for the Ar₁₃ cluster if the heating rate is low since there exists a broad coexistence region

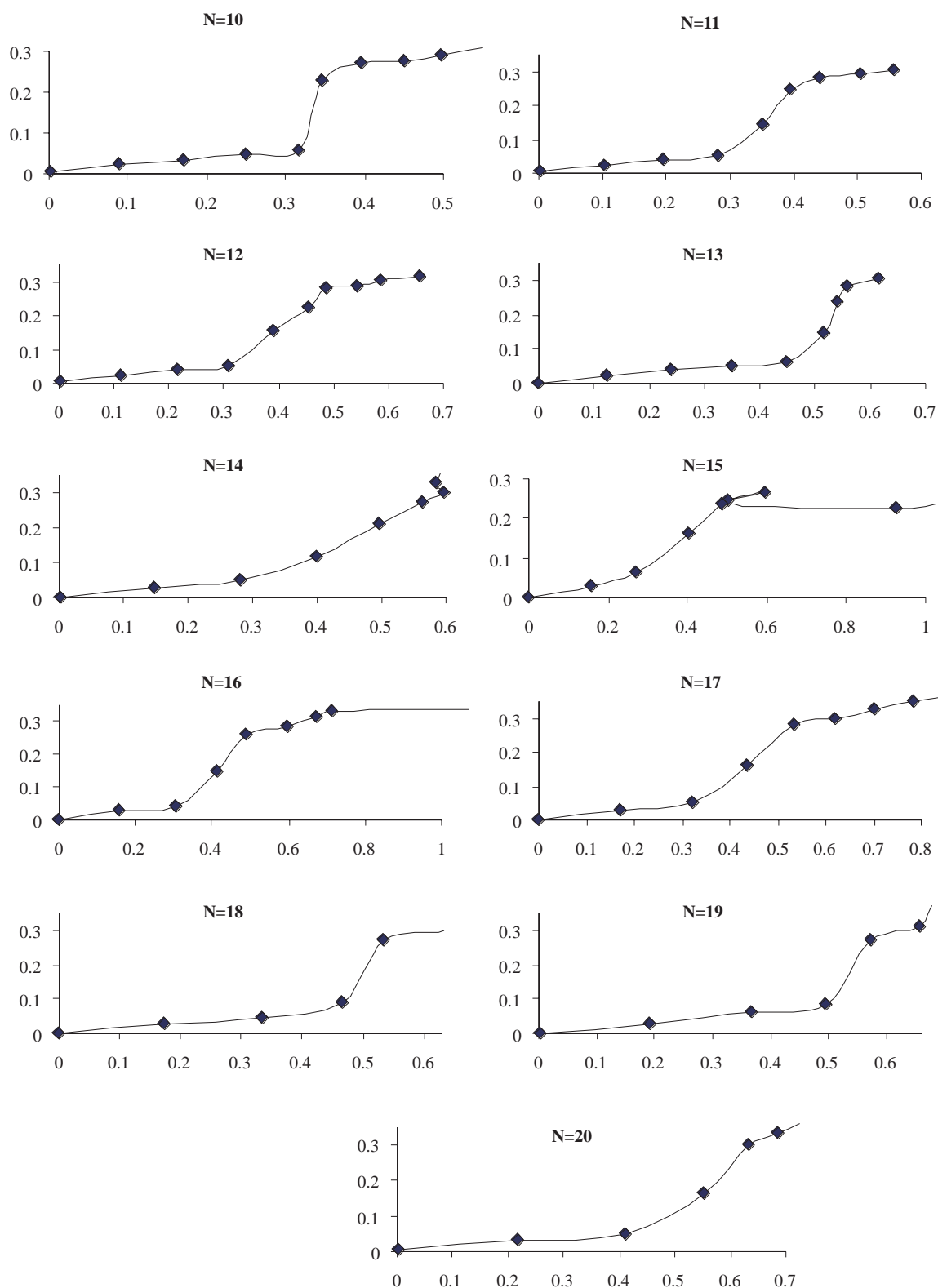


Figure 1. Change in Lindeman factor with average temperature in homogeneous clusters for different cluster sizes. A) N = 10, B) N = 11, C) N = 12, D) N = 13, E) N = 14, F) N = 15, G) N = 16, H) N = 17, I) N = 18, J) N = 19, K) N = 20.

of liquid and solid phases for these clusters. The heating of a cluster system is achieved by increasing the total energy of the system starting from the minimum energy in the constant energy MD simulations. The energy range scanned is also important. In this study, the energy is increased until the liquid phase is obtained or the phase transition curve (δ vs. temperature or δ vs. energy curves) stays almost flat around a δ value, which is above 0.3. For all clusters sizes and for all size ratios, a phase transition is observed. The effect of the size parameter can be observed in Figure 2. For all clusters, the melting point of the homogeneous system is higher than the melting points of the mixtures and it oscillates when σ_B is lowered. The 13-atom cluster is the only one showing a regular increase upon increase of σ_B . In the Table, we present the change in the total energy of the system at the melting point with cluster size (N) and the size of the B component (σ_B).

Table. Change of melting temperatures with N and σ_B .

σ_B	N = 10	N = 11	N = 12	N = 13	N = 14	N = 15
0.50	0.319	0.140	0.220	0.235	0.342	0.444
0.55	0.321	0.283	0.225	0.293	0.255	0.341
0.60	0.275	0.285	0.230	0.253	0.278	0.253
0.65	0.320	0.284	0.257	0.272	0.245	0.225
0.70	0.160	0.196	0.265	0.344	0.320	0.251
0.75	0.093	0.125	0.181	0.418	0.300	0.292
0.80	0.210	0.171	0.264	0.475	0.260	0.270
0.85	0.248	0.130	0.250	0.485	0.275	0.385
0.90	0.300	0.255	0.265	0.517	0.260	0.345
0.95	0.347	0.288	0.345	0.488	0.260	0.400
1.00	0.331	0.350	0.389	0.515	0.440	0.390
σ_B	N = 16	N = 17	N = 18	N = 19	N = 20	
0.50	0.390	0.320	0.290	0.276	0.400	
0.55	0.234	0.375	0.280	0.330	0.407	
0.60	0.272	0.210	0.265	0.360	0.300	
0.65	0.304	0.250	0.275	0.230	0.245	
0.70	0.270	0.248	0.273	0.360	0.300	
0.75	0.400	0.300	0.307	0.272	0.369	
0.80	0.300	0.280	0.346	0.430	0.300	
0.85	0.358	0.300	0.420	0.525	0.400	
0.90	0.400	0.410	0.430	0.552	0.486	
0.95	0.410	0.410	0.440	0.525	0.530	
1.00	0.411	0.437	0.495	0.536	0.553	

In Figures 2 and 3, the change in melting temperature with cluster size and with size ratios is given. The melting points of the N = 13 clusters violate the general tendency that the melting point increases with cluster size, especially in the $0.7 < \sigma_B < 1.0$ region. The A_7B_6 type mixed LJ_{13} clusters are known to have very interesting potential energy surfaces with a large number of close-lying low-energy minima, which are separated by large energy barriers; each of the low-lying structures is one of a set of icosahedra isomers.

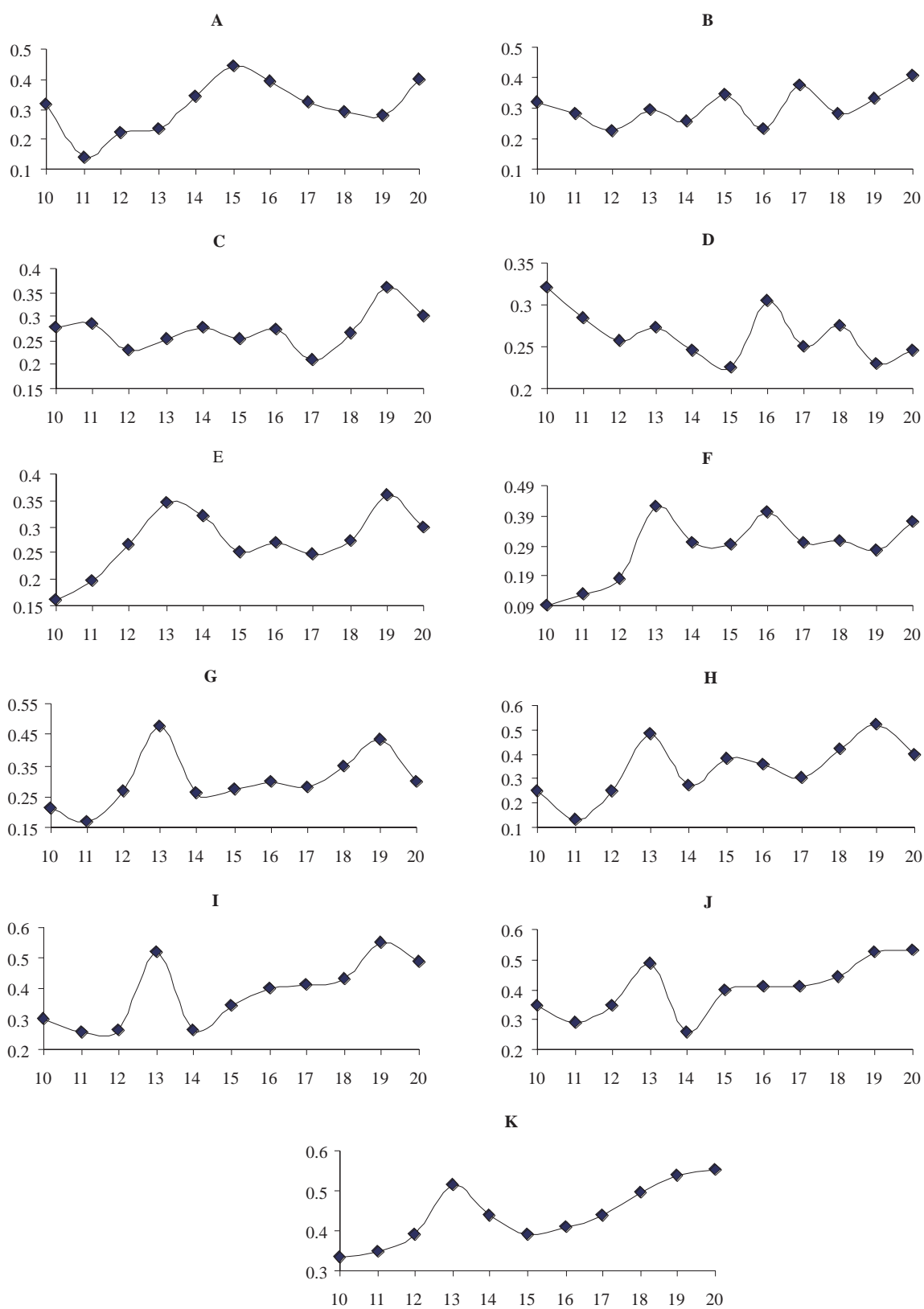


Figure 2. Change in melting temperature with cluster size for A) $\sigma_B = 0.5$, B) $\sigma_B = 0.55$, C) $\sigma_B = 0.6$, D) $\sigma_B = 0.65$, E) $\sigma_B = 0.7$, F) $\sigma_B = 0.75$, G) $\sigma_B = 0.8$, H) $\sigma_B = 0.85$, I) $\sigma_B = 0.9$, J) $\sigma_B = 0.95$, K) $\sigma_B = 1.0$.

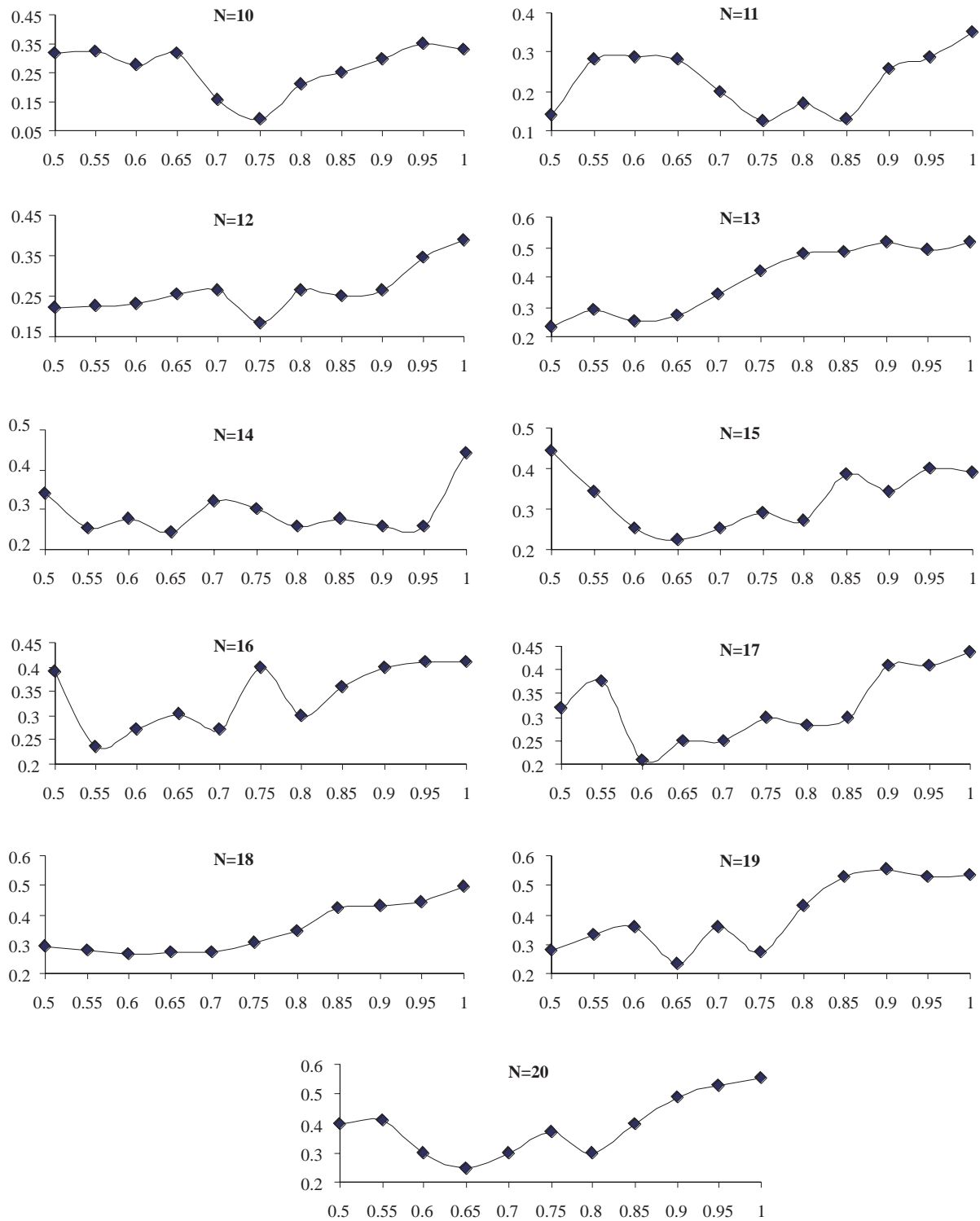


Figure 3. Change in melting temperature with increasing σ_B .

The effect of the ε , the energy parameter of the LJ interaction potential can be seen for 10- and 20-atom clusters in Figure 4. The melting points of the two different clusters show similar trends upon increasing ε . The melting points increase as the $\varepsilon_A/\varepsilon_B$ ratio increases as expected. This increase is sharper for the 20-atom cluster.

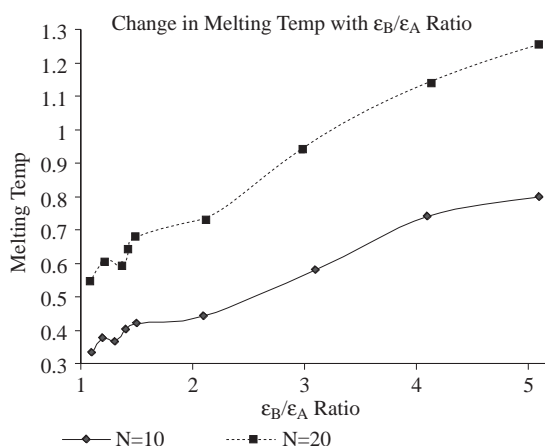


Figure 4. Change in melting point with ϵ_B/ϵ_A

Between the two extremes is a range of energies for clusters at constant energy in which some clusters exhibit a remarkable phenomenon: they spend long intervals of time as solids, then more or less at random jump into the liquid form for rather long periods, then turn back into solids and so on. This is called phase coexistence, which is characteristic for clusters. Some clusters display such coexistence. Coexistence is independent of cluster size. For example, in Ar_{13} clusters, coexistence involves the accessibility of distinct sets of minima with rather different energies. The minima associated with solid-like behavior are more compact and lower in energy, while those associated with liquid-like behavior involve more open structures, which lie higher in energy. Ar_{15} and Ar_{19} clusters give a clear indication of two-phase coexistence but Ar_{17} clusters show both stiff and soft solid forms. To observe phase coexistence behavior, we monitored the short-time averages of the kinetic energy to see whether a bimodal distribution in a finite energy range exists, implying that there is a dynamical coexistence of a hot solid-like phase and a cold liquid-like phase in the above energy range. In this energy range the clusters are supposed to make dynamic excursions between two distinct regions of phase space with different characteristics, solid-like and liquid-like. However, we were unable to see this behavior for all clusters of various sizes and size ratios.

Conclusions

The melting behavior of one component and two component LJ mixtures is studied by classical simulation techniques. Cluster size is varied between 10 and 20. These small clusters are equilibrated at different regions of the microcanonical energy surface starting from the minimum energy configuration. Energy is increased constantly, i.e., the system is heated until melting occurs. The phase transition from solid type phase to liquid type phase is observed by monitoring the Lindemann index (δ). By plotting δ as a function of the average kinetic energy, the melting, temperature of a given cluster is found. When the cluster size is increased, the systems become more stable and the energy is reduced. As a result of this, melting temperature is lowered. The melting temperatures of the finite-sized clusters are said to be higher than those of the corresponding bulk melting temperatures. The melting points of the clusters show no correlation with the energy of initial optimized structures. Clusters show similar trends when one component is smaller than the other. The plots of melting temperature versus size of the component B show no general trends. In these plots one thing is clearly seen: the melting points of the mixtures are approximately the same or lower than those of the homogeneous clusters. The structures of homogeneous clusters go to fcc as the size increases and

fcc corresponds to the packing with the least empty space and the nearest neighbor distances are almost at the minima of the LJ interaction. Therefore, the interactions in the homogeneous clusters are stronger and the melting points are higher. As the heterogeneity increases, the atoms move away from their positions at the minima of the potential. This observation may of course change if the interaction parameter for BB is very large. It is interesting to note that the melting temperature for homogeneous systems ($\sigma_B = 1.0$) or binary mixtures ($\sigma_B < 1.0$) containing 13 atoms behaves differently in the range where σ_B changes between 0.7 to 1.0. These clusters have higher melting points than the rest of the clusters and they have comparable melting points with $N = 20$ clusters. The observed irregularities in melting points for some N values (including $N = 13$) are attributed to the formation of high symmetry structures. Another parameter that affects the melting temperature is the LJ potential parameter, ϵ . If ϵ for one of the component is increased, the average kinetic energy and also the melting temperature are increased. This increase in the temperature is larger for larger clusters. This is, of course, not a surprising result but it gives us the opportunity to test the reliability of the method we used and the numerical results of the simulation. In conclusion, the cluster mixtures melt at lower temperatures than the homogeneous clusters. The effect of the size difference between the atoms in the cluster is not easily predictable for small clusters and it shows oscillatory behavior as a function of size.

Acknowledgments

The authors gratefully acknowledge the I.T.U High Performance Computing Center for providing computer time and the I.T.U. Research Fund for the financial support. We thank David Wales for access to his global minimization program and Ersin Yurtsever for many helpful discussions.

This article was presented at the XI. National Chemistry Congress, İstanbul, Turkey, September, 4-7, 2001.

References

1. R.S. Fellers, C. Leforestier, L.B. Braly, M.G. Brown, R.J. Saykaly, **Science** **284**, 945 (1999).
2. U. Buck, I. Ettischer, M. Melzer, V. Buch, J. Sadlej, **Phys. Rev. Lett.** **80**, 2578 (1998).
3. C.J. Gruenloh, J.R. Carney, C.A. Arrington, T.S. Zwier, S.Y. Fredericks, K.D. Jordan, **Science** **276**, 1678 (1997).
4. K. Natua, R.E. Miller, **Science** **287**, 293 (2000).
5. W.B. Blanton, S.W. Gordon-Wylie, K. Jordan, J.T. Wood, G. Clark, T. J. Collins, **J. Am. Chem. Soc.** **121**, 3551 (1999).
6. P. Ayotte, G.H. Weddle, G.G. Bailey, M. A. Johnson, F. Vila, K.D. Jordan, **J. Chem. Phys.** **110**, 6268 (1999).
7. G.M. Tanner, A. Bhattacharya, S. K. Nayak, and S. D. Mahanti, **Physical Review E** **55**, **1**, 322-328 (1997).
8. S. Berry, *Scientific American* Aug. 50-56 (1990).
9. D.J. Wales and R.S. Berry, **J. Chem. Phys.** **92**, **7**, 4283-4295 (1990).
10. L.J. Munro, A. Tharrington and K.D. Jordan, Preprint (2000).
11. S. Valkealahti and M. Manninen, **Comp. Mater. Sci.** **1**, 123 (1993).

12. A. Rytkonen, S. Valkealahti, and M. Manninen, **J. Chem. Phys.** **106**, **5**, 1888-1892 (1997).
13. B. Vekhter and R.S. Berry, **J. Chem. Phys.** **106**, **15**, 6456-6459 (1997).
14. R.S. Berry, **J. Phys. Chem.** **98**, 6910-6918 (1994).
15. D.J. Wales, **Science**, **271**, 925-928 (1996).
16. F.H. Stillinger, T.A. Weber, **Phys. Rev. A** **25**, 978-989 (1982).
17. F.H. Stillinger, T.A. Weber, **Phys. Rev. A** **28**, 2408-2416 (1983).
18. J. Uppenbrink, D.J. Wales, **J. Chem. Soc. , Faraday Trans.** **87**, 215-222 (1991).
19. W.H. Press, B.P. Flannery, S.A. Teukolsky, W.T. Vetterling, “**Numerical Recipes**”, Cambridge University Press, 1985.
20. J.Q. Sun, K.J. Ruedenberg, **Chem. Phys.** **98**, 9707-9714 (1993).
21. J.Q. Sun, K.J. Ruedenberg, **Chem. Phys.** **99**, 5257-5268 (1993).
22. J.Q. Sun, K.J. Ruedenberg, **Chem. Phys.** **99**, 5269-5275 (1993).
23. J.Q. Sun, K.J. Ruedenberg, **Chem. Phys.** **99**, 5276-5280 (1993).
24. J. Pancik, **Collect. Czech. Chem. Commun.** **40**, 1112-1118 (1975).
25. C.L. Cerjan, W.H. Miller, **J. Chem. Phys.** **75**, 2800-2806 (1981).
26. J. Simons, P. Jorgenson, H. Taylor, **J. Ozment, J. Phys. Chem.** **87**, 2745-2753 (1983).
27. D.O’ Neal, H. Taylor, **J. Simons, J. Phys. Chem.** **88**, 1510-1513 (1984).
28. A. Banarjee, N. Adams, **J. Simons, J. Phys. Chem.** **89**, 52 (1985).
29. J. Baker, **J. Comput. Chem.** **7**, 385-395 (1986).
30. J. Baker, **J. Comput. Chem.** **8**, 563-574 (1987).
31. N. Shida, P.F. Barbara, J.E. Alonlof, **J. Chem. Phys.** **91**, 4061 (1989).
32. H.L. Davis, D.J. Wales, R.S. Berry, **J. Chem. Phys.** **92**, 1173-1182 (1990).
33. R.S. Berry, **In mode selective chemistry**, eds. J. Jortner, A. Pullman, G.B. Pullman, pp. 1-15, Kluwer Academic Publishers, Amsterdam, 1991.
34. R.S. Berry, **Chemical Reviews** **93** (1994).
35. M. Yurtsever, H.Ö. Pamuk, J. Brickmann, **Ber. Bunsenges. Phys. Chem.** **98**, 893-905 (1994).
36. M. Yurtsever, **Turk. J. Chem.** **19**, 151-160 (1995).
37. P.W. Atkins, **Physical Chemistry**, Fifth edition, Oxford University Press.
38. M.P. Allen, D.J. Tildesley, “**Computer Simulation of Liquids**”, Oxford University Press.
39. B.J. Alder, T.E. Wainwright, **J. Chem. Phys.** **27**, 720 (1957).
40. E. Yurtsever, **Phys. Rev. E** **63**, 16202 (2001).
41. J.P.K. Doye and D.J. Wales, **J. Chem. Phys.** **102**, 9673 (1995).
42. J. Jellinek, T.L. Beck, R.S. Berry, **J. Chem. Phys.** **84**, 2783 (1986).